Radiotherapy and Oncology 132 (2019) 70–78

Contents lists available at ScienceDirect

Radiotherapy and Oncology

journal homepage: www.thegreenjournal.com

Original Article

Linac-based radiosurgery for multiple brain metastases: Comparison between two mono-isocenter techniques with multiple non-coplanar arcs

Ruggero Ruggieri [a,*], Stefania Naccarato [a], Rosario Mazzola [a], Francesco Ricchetti [a], Stefanie Corradini [b], Alba Fiorentino [a], Filippo Alongi [a,c]

[a] Department of Radiation Oncology, IRCCS 'Sacro Cuore don Calabria', Negrar (VR), Italy; [b] Department of Radiation Oncology, University Hospital, LMU Munich, Germany; [c] University of Brescia, Italy

ARTICLE INFO

Article history:
Received 5 July 2018
Received in revised form 20 November 2018
Accepted 22 November 2018
Available online 21 December 2018

Keywords:
SRS
VMAT
Brain metastases
HyperArc
MultipleBrainMets

ABSTRACT

Background and purpose: Three mono-isocenter techniques with multiple non-coplanar arcs are nowadays clinically available for linac-based stereotactic radiosurgery (SRS) of multiple brain metastases (BM): HyperArc (HA), Multiple Brain Mets (MBM), and Monaco-HDRS. Two of them, HA and MBM, are here compared in terms of plan-quality, and dosimetric consistency between planning and delivering.

Materials and methods: For 20 patients with multiple BM (2–10), treated by mono-isocenter volumetric modulated arc therapy (VMAT) HA plans, mono-isocenter MBM dynamic conformal arc plans were generated. Prescription dose (Dp) was 18–25 Gy, for single-fraction, and 21–27 Gy, for three-fractions. Mean overall Planning Target Volume (PTV), expanded by 2 mm from each lesion, was 9.6 cm^3 (0.5–27.9 cm^3). Dose normalization of 100%Dp at 98%PTV was adopted. Plan-quality was compared by the Paddick conformity (CI) and gradient (GI) index, for the target, mean dose and V_{12} volume, for the healthy brain, and number of monitor units (MU). Further, verification dosimetry by radiochromic films was performed for each plan, thus comparing also, by γ-analysis, the consistency between in-phantom computed and measured dose distributions.

Results: CI significantly improved for HA plans, changing on average from 0.75 (MBM) to 0.94 (HA) ($p < .001$). No significant differences between HA and MBM plans were computed for GI ($p = .216$), and for mean dose ($p = .436$) and V_{12} ($p = .062$) to the healthy brain; although V_{12} increased on average from 23.7 cm^3 (HA) to 37.3 cm^3 (MBM). No significant difference resulted for MU ($p = .107$), whereas γ (1 mm, 3%) and γ (2 mm, 2%) passing-rates significantly improved for HA plans ($p = .006$; $p = .023$).

Conclusions: HA plans assured a higher CI, while no significant difference resulted for any of the other planning metrics. Although on average slightly higher for HA plans, the dosimetric consistency between planned and delivered was satisfactory from both techniques. Hence, our judgement of near equal plan-quality from HA and MBM SRS-techniques.

Brain metastases BM are the most common intracranial tumors in adults: about 20–40% of cancer patients will develop BM in their oncological history [1]. In the past, patients with multiple BM were typically treated by whole-brain radiotherapy (WBRT). Radiosurgery, both as single-fraction (SRS) and as 3–5 fractions (FSRT) stereotactic radiotherapy, has also gained importance in this treatment setting [2], given the increased risk of detriment in neurocognitive functions for patients undergoing WBRT [3,4], without any improvement in overall survival (OS) as compared to SRS/FSRT [5,6]. Although SRS is now widely used for patients with ≤4 BM [5,7], Yamamoto et al. [8] have shown similar OS for patients with 5–10 BM when compared to patients with 2–4 BM, thus suggesting that the use of SRS/FSRT may be appropriate even in patients with up to 10 BM [9]. Such a clinical framework created the need for a technical solution which, while reproducing for multiple BM similar dose-gradient steepness and target dose conformity to single-lesion SRS, could be performed within 20 min at the treatment machine.

For linacs, a mono-isocentric approach by multiple non-coplanar arcs was then proposed. Treatment time was shortened enough, because the use of one isocenter involves one IGRT session, but the use of large fields, to cover many distinct lesions, also posed optimization problems for the kinetics of the leaves of the

* Corresponding author at: IRCCS 'Sacro cuore don Calabria', Via don A. Sempreboni 5, 37024 Negrar, VR, Italy.
E-mail address: ruggero.ruggieri@sacrocuore.it (R. Ruggieri).

https://doi.org/10.1016/j.radonc.2018.11.014
0167-8140/

multi-leaf-collimator (MLC), which were initially solved by in-house made solutions [10–13]. Nowadays, although most of the existing treatment planning systems (TPS) allow to optimize a mono-isocentric plan of multiple BM by multiple non-coplanar arcs through a planner-dependent choice of several geometric parameters (number/extent of arcs, couch/collimator angles), three commercial solutions exist which offer at this purpose specific forms of automation: HyperArc™ (HA) (Varian Medical System, Palo Alto, CA), which is a development of the volumetric modulated arc therapy (VMAT) approach first proposed by Clark et al. [10–12]; MultipleBrainMets™ (MBM) (Brainlab AG, Munchen, Germany), which adopts a dynamic conformal arc approach [13]; and Monaco HDRS (Elekta AB, Stockholm, Sweden).

Purpose of the present analysis was to compare the plan quality of two of such techniques, HA and MBM, both in terms of computed dose and efficiency metrics, and in terms of consistency between in-phantom planned and delivered dose distributions. Considerations about the distinct IGRT approaches proposed from the distinct producers of HA and MBM techniques, although setup accuracy being of great relevance for this type of treatments, were not included in the present analysis.

Methods

Patients

20 patients with multiple BM (mean 5, range 2–10), treated by SRS/FSRT in 1–3 fractions by HA as previously described [14], were selected for this Institutional Review Board (IRB) approved retrospective dosimetry study, which included informed consent from all patients. The prescription doses (D_p) were: 18–25 Gy in single-fraction (for BM diameters <3 cm) [15]; and 21–27 Gy in three-fractions (for BM >3 cm, or adjacent to critical structures) [16]. Patients' data are summarized in Table 1. Treatments were performed on a TrueBeam™ (Varian Inc.) linac, with 10 MV flattening-filter-free photon beam and a Millenium 120-leaves MLC, whose only central leaves (0.5 cm at isocenter) have been used in our plans.

Planning-CT (CTp) of supine patients, within the Encompass™ (QFix, Avondale, PA – USA) mask and support, were scanned (1 mm slice thickness) without contrast medium. Gross tumor volumes (GTV) and organs at risk (OAR) were contoured on MRI scans (3D spoiled-GRE T1). The clinical target volume (CTV) was assumed equal to GTV. Planning target volume (PTV) was expanded by 2 mm from CTV, to improve dosimetric accuracy as well as to minimize the risk of geographical miss [17,18]. A zero margin for PTV would translate into smaller equivalent field size per control point and into likely underestimated output factors: which, in turn, would translate into likely overestimated MU, for the smallest lesions at least. Correspondingly, the difference between measured and computed dose per lesion would increase with lesion-size reduction. Although the risk of geographical miss of small BMs due to uncorrected rotational errors [19] differentially impacts on the BMs according to their distance from the isocenter, we cautiously adopted the same 2 mm margin also for central (to the isocenter) lesions. The OARs were: brain-minus-PTV (BmP), eyes, lenses, optic chiasm, optic nerves, brainstem and hippocampi. For planning approval of single fraction (three-fractions) SRS the near-maximum dose ($D_{0.5cm3}$) had to be lower than 10 (18) Gy, for the brainstem, and lower than 8 (15) Gy, for the eyes, lenses, optic chiasm, and optic nerves. Further, mean dose to the hippocampi had to be lower than 5 (7) Gy [20].

In this study, one D_p value was used for all the lesions of each patient, and volumetric dose prescription was 100%D_p to 98% of the union of all PTVs (PTV_all). Further, $D_{2\%}$(PTV) as large as 150%D_p was accepted, because the practice of limiting intra-tumor dose heterogeneity was negatively associated with a reduced CI and increased V_{12} and GI [21].

Table 1
Demographics and clinical characteristics of study patients (8/20 M, 12/20 F).[a]

	Mean	St. dev.	Min	Max
Age (y)	58	10	37	77
N. lesions	5	2	2	10
d_i (cm)	5.5	1.7	2.7	8.2
PTV_all (cm^3)	9.6	8.1	0.5	29.0
PTV (cm^3)	2.0	2.9	0.1	18.6
D_p (Gy)	25.0	2.5	18	27
N. fractions	2.3	1.0	1	3

[a] M, male; F, female; *st. dev.*, standard deviation; *N.*, number of; d_i, per-patient average distance from isocenter of each lesion; *PTV_all*, total planning target volume; *PTV*, single lesion planning target volume; *Dp*, prescription dose.

HA and MBM plans

Both techniques position the isocenter at the centroid of the set of lesions. HyperArc™, an add-on of the Eclipse™ (v. 15.5.07, Varian Inc.) TPS, adopts the class-solution from Clark et al. [11,12], with a maximum of 5 non-coplanar 180°-arcs, based on 4 of 5 possible angular couch positions (0°, ±45°, ±90°) (Fig. 1A). By a digital model of the linac head, HA estimates the clearance between the patient and the machine for any couch position. As previously described [14], HA integrates its VMAT optimizer (PO) by three dedicated algorithms which optimize the collimator angle per arc (CAO), the sharpness of the dose fall-off to the surrounding BmP (SRS-NTO), and the simultaneous dose coverage of each target (ALDO).

MultipleBrainMets™ (v. 1.5, Brainlab AG), which is an add-on of Elements™ (Brainlab AG) TPS, geometrically optimizes the couch angles (here pre-selected from the planner in the numbers of 5 and 6, where the best performing of such two plans was next used for comparison with the HA plan for the same patient), to avoid opposing arcs, the arc lengths, to minimize ocular involvement (Fig. 1B), the collimator angles, to avoid inter-lesions dose bridges, and the field extensions, to minimize the number of monitor units (MU) by including as many lesions as possible but not all of them. Finally, any arc weight is optimized to improve target dose conformity.

Dose distributions were computed, with 1 mm of dose-grid step and 2 degrees of angular step (control point) along the arcs, by different dose calculation algorithms: AAA (v. 15.5.07, Varian Inc.) for HA, and a pencil-beam based one for MBM. Although such two algorithms have different accuracy in dose prediction at tissue inhomogeneities, this is not a major issue for cranial irradiation by multiple arcs, at least for lesions which are not abutted to the base of the skull, since most of the perturbation effect of the cranial bone is compensated by the multiple beam arrangement [22]. HA and MBM also differ in optimization: inverse planning for HA, whereas optimal weighting of conformal arcs, after the above reported geometric optimizations, for MBM. As a result, the dose-rate along the arcs is variable in HA but constant in MBM, and, mostly, the mean aperture between opposing leaves per control point can be very small in HA, whereas enlarged to a similar size to the treated lesions in MBM.

In-phantom dosimetric verifications (iPDV)

To test if such different complexity of the irradiation, in terms of dose rate and leaf positional accuracy per control point, might impact on the accuracy of dose delivery, a comparison in terms of γ-analysis [23] of in-phantom dosimetric verifications (iPDV) of HA and MBM plans was conceived. At this purpose, all patients' plans were recomputed (1 mm dose-grid step, and 2 degrees

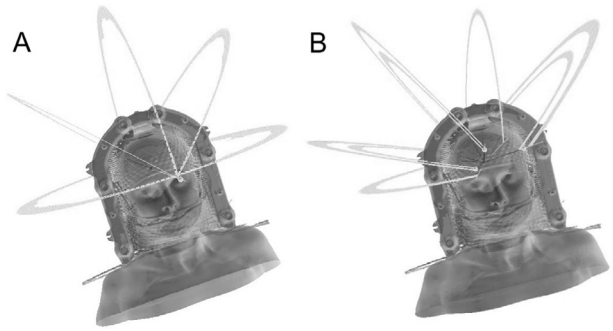

Fig. 1. Typical beam arrangements for HA (A) and MBM (B) plans. Whereas in HA plans couch positions (0°, ±45°, ±90°) and arc extensions (180°) are fixed, their values result from patient-specific optimization in MBM plans.

angular step) in the Octavius™ (PTW GmbH, Freiburg, Germany) phantom (Fig. 2). Although the accuracy of couch rotation is routinely verified by a test from the linac vendor ('MPC enhanced couch': an extension of a previously reported test [24]), whose tolerance for the disalignment between radiation and couch-mechanical isocenters is as strict as 0.75 mm, the above recomputations were done with the same couch rotations as in the original patient plan to fully simulate the treatment setting. For each one of the twenty patients, after the planned isocenter was vertically adjusted in Octavius™ phantom so as to assure that the plane of the gafchromic-film (EBT3™, Ashland SI, Bridgewater, NJ) detector included the maximum number of almost coplanar lesions, thus testing the whole dose range, two distinct films were irradiated, one for the HA and one for the MBM plan, for a total of forty irradiated films. EBT3 films (lot# 12121702) were calibrated soon before their use for iPDV, scanned at 72 dpi 17 hours after irradiation, by an Expression 10000XL (Epson Inc.) flat-bed scanner, and converted in RGB (tiff) images. Film calibration was performed by the 10 MV with-flattening-filter photon beam from the same linac used for treatments, to assure large enough regions of homogeneous dose. Further, ten levels of dose (plus zero) were used, which were sampled along a geometric progression until 24 Gy,

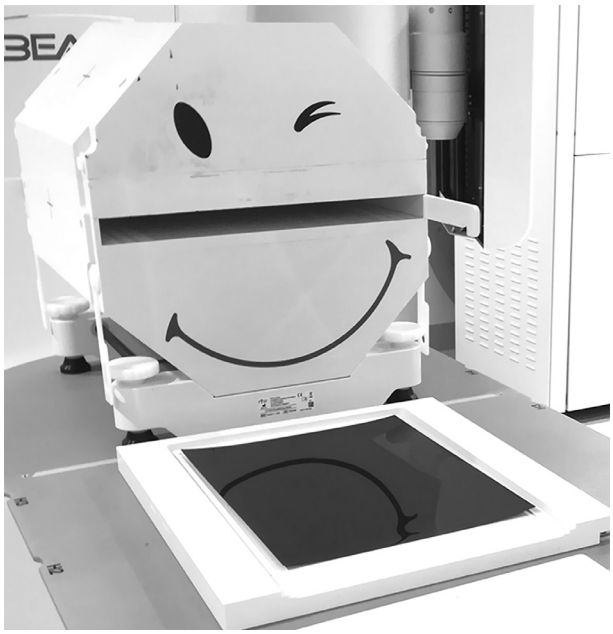

Fig. 2. The Octavius™ phantom (PTW GmbH) with the insert (here extracted) for the gafchromic film positioning.

i.e. until 1.2 times the maximum in-phantom computed dose, on the film plane, over all patients plans. Optimized dose maps were computed, by a triple-channel color-to-dose calibration [25], in 'Film QA Pro 2014' (Ashland SI Inc.) software and then exported, in the red-channel only, for film maximum dose <10 Gy, or the green channel only, for film maximum dose >10 Gy, similarly to [26]. γ-Index computation for consistency between film-measured and TPS computed dose matrixes was then performed by 'Verisoft 4.2' (PTW GmbH) software, with thresholds in relative dose-difference (DD) and in distance-to-agreement (DTA) of (2 mm, 2%) [27] and (1 mm, 3%) [26]. The latter criterion implies a spatial resolution of at least 1/3 mm [29], hence the choice of the gafchromic-film high resolution detector scanned at 72 dpi. DD was normalized both to the locally computed dose (^{local}), and to the maximum computed dose (^{Max}), the latter avoiding unrealistic dose accuracy requirements in the low-dose regions [29] for the most stringent 1 mm DTA threshold. Pixels with computed doses lower than 20% of the maximum dose were neglected for γ-index estimation.

Comparison metrics

Since a correlation between the extent of intermediate dose spill (e.g., the volume receiving at least 12 Gy: V_{12}) to the BmP and the risk of radionecrosis was reported for cranial SRS/FSRT [30–32], V_{12}(BmP) was used as a metric of plan quality. The mean dose (D_{mean}) of BmP also was analyzed, being its minimization advisable in patients with high re-treatment rates like those ones with multiple BM treated by SRS.

For target dose coverage, both the Paddick conformity index (CI), and the Paddick gradient index (GI) were used [33]. CI is defined by CI = (PTV_{Dp}/PTV)* (PTV_{Dp}/V_{Dp}), where PTV_{Dp} is the fraction of PTV covered by the prescription isodose, and V_{Dp} is the prescription isodose volume (cm^3). Given our dose normalization, PTV_{Dp}/PTV = 0.98, CI reduces to 0.98*(0.98* PTV/V_{Dp}). Being GI = $V_{50\%Dp}$/V_{Dp}, it describes the steepness of the dose gradient from high (D_p) to medium (50%D_p) dose levels.

The values of the above planning metrics, for both HA and MBM plans, were deduced from the recomputed DVHs by a 3rd part RT-Dicom viewer (DICOMan^{TX} v. 4.8.6, http://radonc.uams.edu/research/dicoman/): this was done to avoid any potential imbalance which might had occurred if such same recomputations had been done in any of the two here compared TPS, Eclipse™ or Elements™.

The total number of monitor units (MU) per fraction was used as indicator of irradiation efficiency. As indicators of accuracy in dose delivery, the passing-rate (PR) of γ-index with test criterions of (1 mm, 3%) and (2 mm, 2%) were used with global, PR^{Max}(1 mm, 3%), and local, PR^{local}(2 mm, 2%), dose normalization [29,34] respectively.

Statistics

For each one of the above metrics, the two HA and MBM samples were first tested for normality of distribution by Lilliefors' test [28]. Then, according to the results of such preliminary test, each couple of samples was compared by a non-parametric Wilcoxon signed-rank test, or by a parametric *t*-test. All computations, including linear regression analysis, at the 0.05 level for statistical significance, were performed by XLSTAT (v. 7.5.2, Addinsoft Inc.) add-on for Excel™ (Microsoft Inc.).

Results

All values of the compared metrics, for both RA and MBM plans, are listed: in Table 2 for V_{12}(BmP), D_{mean}(BmP), CI, GI, and MU; in

Table 2
Values of the plan quality metrics and results from hypothesis testing.[a]

	D^{BmP}_{mean} (Gy)		V^{BmP}_{12} (cm^3)		CI		GI		MU	
Pt.#|Plan	HA	MBM	HA	MBM	HA	MBM	HA	MBM	HA	MBM
1	2.74	2.90	5.9	11.9	0.90	0.78	4.55	5.09	6605	5767
2	2.46	2.62	8.9	16.8	0.86	0.80	4.35	5.79	7600	9709
3	2.97	3.49	29.3	44.1	0.93	0.68	3.36	3.29	2345	1974
4	5.25	6.64	46.4	89.9	0.94	0.77	3.41	4.13	3202	3631
5	1.71	1.69	7.7	10.4	0.99	0.96	4.04	4.61	6813	4677
6	1.70	1.66	12.3	14.8	0.97	0.82	3.59	3.49	2230	1770
7	2.15	2.29	9.9	14.6	0.98	0.70	4.68	4.45	6236	6783
8	2.15	2.11	13.3	18.6	0.95	0.85	4.06	4.56	2420	2299
9	2.84	3.20	20.5	29.9	0.97	0.70	3.77	3.61	2222	2281
10	4.02	4.35	25.1	40.3	0.96	0.77	3.32	3.41	2928	2114
11	1.87	1.63	6.1	8.0	0.95	0.74	4.38	4.30	2779	2069
12	0.76	0.85	1.7	3.2	0.85	0.40	7.46	5.49	2311	2034
13	4.61	4.83	31.3	49.7	0.92	0.64	3.82	3.70	3336	3060
14	6.17	7.34	86.6	157.5	0.92	0.58	4.71	4.87	3842	3872
15	1.83	1.90	13.9	19.5	0.98	0.78	3.45	3.44	5598	4053
16	1.43	1.42	7.5	10.8	0.95	0.88	3.75	4.35	2256	1664
17	2.92	2.82	13.8	20.7	1.00	0.81	3.91	4.17	7843	6527
18	2.97	2.87	11.5	17.4	0.95	0.86	4.79	5.71	8976	7376
19	3.47	3.48	41.2	57.1	0.95	0.78	3.54	3.51	2598	2191
20	5.77	6.30	80.4	110.4	0.92	0.70	4.39	4.23	4197	3027
Mean	2.99	3.22	23.7	37.3	0.94	0.75	4.17	4.31	*4317*	*3844*
Sd	1.49	1.82	23.7	39.8	0.04	0.12	0.91	0.78	*2247*	*2271*
Min	0.76	0.85	1.7	3.2	0.85	0.40	3.32	3.29	*2222*	*1664*
Max	6.17	7.34	86.6	157.5	1.00	0.96	7.46	5.79	*8976*	*9709*
	$p = .871^{§}$ $p = .436^{‡}$		$p = .123^{§}$ $p = .062^{‡}$		$p < \mathbf{.001}^{*}$ $p < \mathbf{.001}^{†}$		$p = .433^{§}$ $p = .216^{‡}$		$p = .213^{§}$ $p = .107^{‡}$	

Bold characters are used for *p*-values when statistical significance resulted ($p < .05$) from 2-tails (§), or 1-tail (‡) *U* Mann–Whitney's test, or from 2-tails (*), or 1-tail (†) *t*-test.
[a] D^{BmP}_{mean} (Gy), mean dose to healthy brain; V^{BmP}_{12} (cm^3), percentage volume of healthy brain receiving no less than 12 Gy; *CI*, conformity index; *GI*, gradient index; *MU*, monitor units per fraction; *sd*, standard deviation.

Table 3 for PR^{Max}(1 mm, 3%) and PR^{local}(2 mm, 2%). In each table, the results from hypothesis testing are also reported.

The only statistically significant improvement in favor of HA plans was achieved for CI, whose (mean ± sd) value increased from (0.75 ± 0.12), for MBM plans, to (0.94 ± 0.04), for HA plans ($p < .001$).

No significant difference resulted for GI, which was equal to (4.31 ± 0.78) for MBM plans, while (4.17 ± 0.91) for HA plans ($p = .216$). No significant difference resulted for D_{mean}(BmP), which was equal to (3.22 ± 1.82) Gy for MBM plans, while (2.99 ± 1.49) Gy for HA plans ($p = .436$). Consistently with the equivalence in GI values, no significant difference resulted for V_{12}(BmP), which was equal to (37.3 ± 39.8) cm^3 for MBM plans, while (23.7 ± 23.7), for HA plans ($p = .062$). Noteworthy, although not statistically significant, HA plans assured an about 37% average reduction in V_{12}(BmP).

In Figs. 3–4 the average cumulative dose–volume histograms (cDVH) are reported for PTV_all (Fig. 3) and BmP (Fig. 4, sub-plot A), by mean curve and (± 1 sd) inter-patient variation bars, for the most numerous subgroup sharing the same dose prescription (i.e., 9 Gy x3fr., for 9/20 patients). In Fig. 3 further cDVH(PTV) curves were overlaid for comparison, and zoomed in the dose range where variations exist. First, the effect of target size on PTV dose heterogeneity was estimated by comparing the HA and MBM plans of both the smallest (4 small lesions [from 0.1 to 0.2 cm^3], for a total PTV = 0.5 cm^3), and the largest (10 variable size lesions [from 0.8 to 6.2 cm^3], for a total PTV = 21.7 cm^3) PTV_all. Whereas for the smallest PTV_all almost no difference resulted between HA and MBM plans in terms of intra-tumor dose heterogeneity ($D_{2\%}$), the opposite was true for the largest volume, where the difference in $D_{2\%}$ was larger than on average. It seems that dose-modulation, in terms of steepness of dose-gradients around the lesions, from HA plans increases with an increasing size from each lesion and, hence, from PTV_all.

To analyze in more details the impact on the cDVH(BmP) curves for the HA and MBM plans from factors like the size of PTV_all, and the product of the number of lesions (N) by the per-patient average distance from the isocenter of each lesion (d_i), as estimate for target geometric complexity, in Fig. 4.B four different patient cases were compared. The first two cases (#12, #9) show that when PTV_all increases, from 0.5 cm^3 to 7.2 cm^3, at a substantially constant product of N for d_i (Nd_i), a systematic drift of the cDVH (BmP) curves toward higher doses is similarly determined for both HA and MBM plans. Further, a similar drift toward higher doses for both HA and MBM plans results by comparing the third (#19: 19.6 cm^3) and the fourth (#20: 21.7 cm^3) cases, i.e. at almost constant size for PTV_all but with increasing Nd_i (from 3x 3.4 cm, #19, to 10× 5.8 cm, #20). Both quantities, PTV_all and Nd_i, seem then determining the level of dose sparing which is achievable from the here conceived HA and MBM techniques.

According to irradiation efficiency, no significant difference resulted in the number of MU per fraction: equal to (3844 ± 2271) MU for MBM plans, while (4317 ± 2247) MU for HA plans ($p = .107$).

In terms of accuracy of dose delivery, statistically significant differences were found for both PR^{local}(2 mm, 2%) and PR^{Max}(1 mm, 3%), although all plans from both groups assured a PR ≥ 90% (PR^{Max} (1 mm, 3%) ≥ 90% is our minimum criterion for the clinical usage of the plan) for both metrics. In details, PR^{Max}(1 mm, 3%) was equal to (98.2 ± 2.9)% for HA plans, while (96.4 ± 3.5)% for MBM plans ($p = .023$), and PR^{local}(2 mm, 2%) was equal to (97.0 ± 1.9)% for HA plans, while (94.9 ± 3.0)% for MBM plans ($p = .006$).

In Fig. 5 a comparison of in-phantom computed and measured absolute dose profiles (subplots A-D), together with the corresponding dose (E-F) and γ (1 mm, 3%) (G-H) maps, is presented for a patient (#20) with 10 lesions, with 5/10 hot spots from the computed dose distribution which were at least partially captured from the chosen plane of measurement. Even with so many lesions,

Table 3
Globally (^{Max}) and locally (^{local}) normalized passing-rates (PR) for γ (1 mm, 3%) and γ (2 mm, 2%) from in-phantom dosimetric verifications, and results from hypothesis testing.[a]

	PR^{Max}(1 mm, 3%)		PR^{local}(2 mm, 2%)	
Pt.#|Plan	HA	MBM	HA	MBM
1	90.2%	90.4%	93.3%	90.0%
2	99.1%	98.2%	97.8%	95.8%
3	100.0%	94.6%	99.0%	98.3%
4	98.5%	94.3%	94.6%	92.0%
5	96.5%	93.6%	96.5%	92.6%
6	99.0%	96.4%	99.2%	97.9%
7	92.0%	90.7%	98.2%	91.8%
8	100.0%	97.6%	98.1%	93.7%
9	100.0%	100.0%	96.7%	98.9%
10	100.0%	100.0%	99.4%	98.1%
11	100.0%	99.7%	98.0%	97.0%
12	100.0%	100.0%	96.5%	97.0%
13	100.0%	99.4%	96.3%	98.0%
14	99.8%	97.0%	92.5%	92.0%
15	97.8%	90.7%	98.9%	90.0%
16	100.0%	100.0%	96.0%	97.7%
17	99.6%	97.6%	96.6%	95.3%
18	93.2%	91.1%	96.1%	90.4%
19	99.1%	98.2%	99.1%	95.0%
20	98.4%	97.8%	96.3%	95.6%
Mean	*98.2%*	*96.4%*	*97.0%*	*94.9%*
Sd	*2.9%*	*3.5%*	*1.9%*	*3.0%*
Min	*90.2%*	*90.4%*	*92.5%*	*90.0%*
Max	*100.0%*	*100.0%*	*99.4%*	*98.9%*
	$p = .047^{\S}$ $p = .023^{\ddagger}$		$p = .031^{\dagger}$ $p = .006^{*}$	

[a] *sd*, standard deviation. Bold characters are used for *p*-values when statistical significance resulted ($p < .05$) from 2-tails (§), or 1-tail (‡) *U* Mann–Whitney's test, or from 2-tails (†), or 1-tail (*) *t*-test.

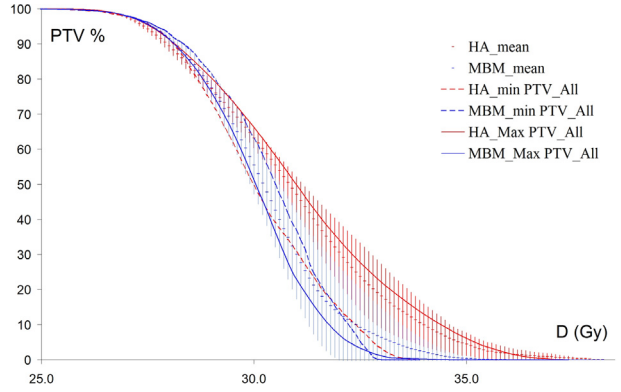

Fig. 3. Cumulative dose–volume histograms (cDVH) of PTV_All, from HA (red-light) and MBM (blue-dark) plans, depicted by the mean curve and its (± 1 sd) variation bars, for the most numerous sub-group of patients (9/20) sharing the same dose prescription (9 Gy x3fr.). The curves for the smallest (0.5 cm^3), and the largest (21.7 cm^3) PTV_all in this sub-group were overlaid for comparison.

for both HA and MBM plans (PR^{Max}(1 mm, 3%) = 98.4% (HA); 97.8% (MBM)) the consistency between planned and measured dose distributions was adequate.

We finally tested if the increased plan complexity which is associated firstly with an increased N, and secondly with an increased product Nd_i, might impact on the accuracy of dose delivery. At this purpose, we first stratified our in-phantom dosimetric verifications according to N – $N \leq 3$ (9/20), and $N \geq 4$ (11/20) –, and hence compared between such two groups, for both HA and MBM plans, PR^{Max}(1 mm, 3%) and PR^{local}(2 mm, 2%). Although statistical significance was reached for the variation (−1.9%) in PR^{Max}(1 mm, 3%) for HA plans ($p = .017$) only, a reduction in both passing rates for the group of patients with $N \geq 4$ (range: 0.7–1.9%) occurred on average for both HA and MBM techniques. Further, by linear

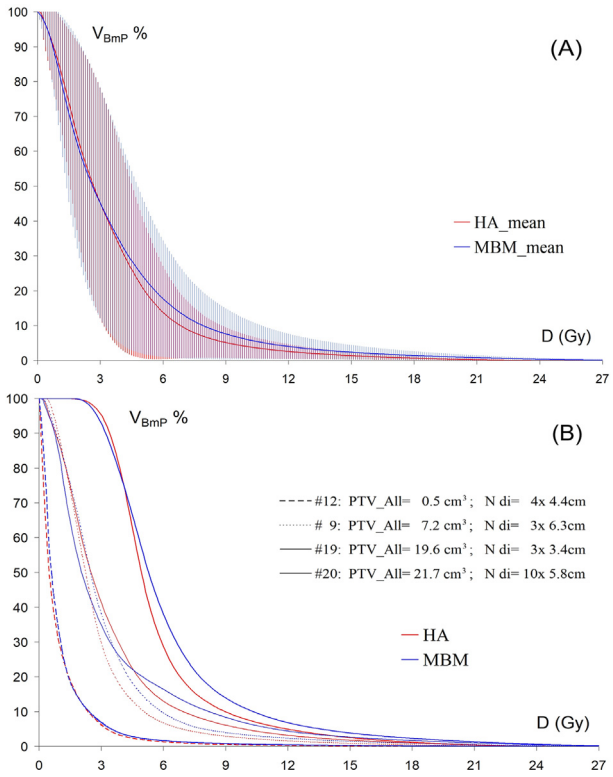

Fig. 4. Cumulative dose–volume histograms (cDVH) of BmP, from HA (red-light) and MBM (blue-dark) plans, depicted by the mean curve and its (± 1 sd) variation bars (sub-plot A), for the most numerous sub-group of patients (9/20) sharing the same dose prescription (9 Gy x3fr.). Sub-plot B depicts four patient cases, as detailed in the legend in terms of individual PTV_All and product of the number of lesions (N) for the mean distance between lesions and isocenter (d_i).

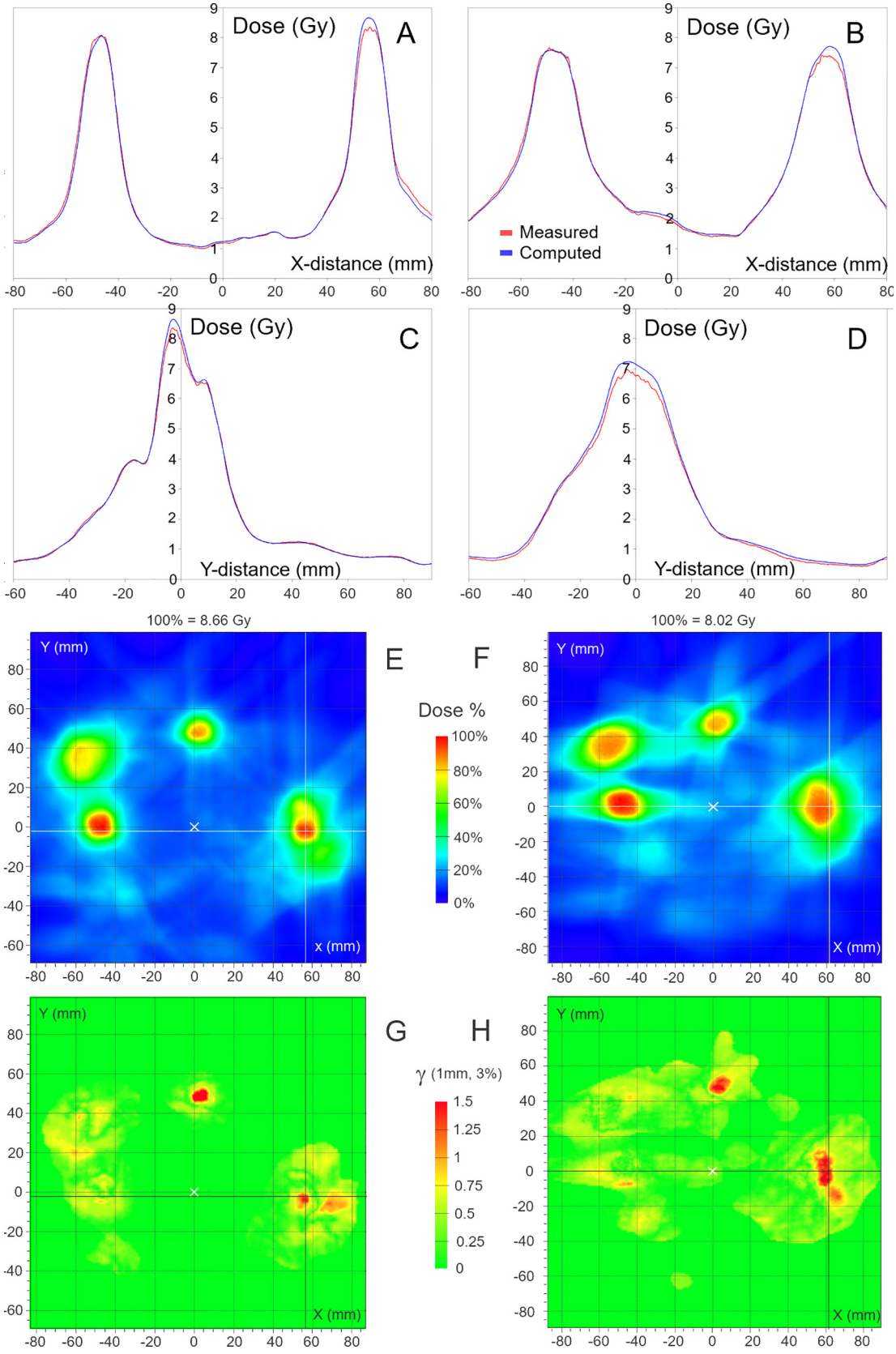

Fig. 5. For the HA plan, in the first column (A, C, E, G), and the MBM plan, in the second column (B, D, F, H), of an example patient (#20, with 5/10 lesions crossing the measurement plane), in-phantom comparisons are depicted for: X-transversal (A, B) and Y-longitudinal (C, D) absolute dose profiles; XY-maps of dose (E, F) and of γ (1 mm, 3%) (G, H) values, with correlation bars to explain the color-wash (100% of absolute dose is distinctly specified for the two plans), and a white cross to indicate the isocenter projection. The couples of normal lines on dose (white) and γ-values (black) maps, which were chosen to explore a region with $\gamma > 1$, identify the spatial location of the corresponding 1D dose profiles in (A-D).

regression analysis of $Y = PR_{HA}^{Max}(1\,mm, 3\%)$ as a function of $X = Nd_i$, $R^2 = 0.268$ and $p = .019$ from t-testing ($\alpha = 0.05$) of the explicative power of X over Y, for an angular coefficient of −0.6%/10 cm, resulted.

Discussion

Due to the ongoing paradigm-shift from WBRT to SRS/SFRT, the need for stereotactic techniques of multiple BM which are fast and reliable at both the planning and the treatment side is growing up. At this purpose, a linac-based mono-isocenter approach by multiple noncoplanar arcs was conceived [10–13], with the potential of a widespread diffusion for linac users. Here we compared two of the three currently commercially available approaches of such a type which include some form of automation, HyperArc™ (Varian Inc.) and MultipleBrainMets™ (BrainLab AG), in terms of both the quality of the planned dose distribution and its consistency with the in-phantom delivered dose. A further inter-comparison study involving the untested third solution, Monaco-HDRS (Elekta AB), is currently under consideration.

Plan quality

For single lesion SRS/SFRT reference values for the metrics of the quality of the planned dose distribution were reported. For the CI index, which impacts on the probability of local control and the sparing of an adjacent serial OAR, typical values for single lesion SRS were around 0.80–0.85 [33]. For multiple lesions, however, a CI value >0.70–0.75 might be enough, consistently with previous studies on VMAT with multiple-noncoplanar-arcs: mean reported CI were 0.76 with 3 BM [10], and 0.74 with 2 BM [35]. Consequently, the statistically significant difference in CI we observed between HA (0.94 ± 0.04) and MBM (0.75 ± 0.12) plans, might be not so clinically relevant, except for cases with metastases which are strictly adjacent to, or even overlapping with, a critical serial OAR.

For all the remaining dose–volume metrics, consistently with the similarity between the color wash dose maps reported in Fig. 6 for a 10-metastases case (#20), such as for the efficiency in irradiation (i.e., MU per fraction), no significant difference resulted between HA and MBM plans. This supports a judgement of substantial equivalence in plan quality from the two techniques.

Some useful hints may be deduced for the optimal values of some metrics. For the GI index, a value not larger than 3 was suggested since Paddick et al. [33] in case of single-lesion SRS. For SRS of multiple BM a larger optimal GI is awaited. Our mean GI values (4.17 for HA, and 4.31 for MBM plans) are consistent with the 4.77 mean value reported for 3–4 BM [36], and with the 4.4 median value reported for a median of 5 BM [37]. Therefore, an optimal GI value around 4–4.5 seems reliable, as a function of the number-of/distance-between lesions and their absolute volumes.

Any reduction in GI directly translates into a reduction in V_{12}(BmP), which is related to the risk of radionecrosis [30–32]. Mean V_{12}(BmP) values from both HA and MBM plans were quite larger than the generally recommended 10 cm^3 threshold for single lesion SRS [30–32]. However, if the ratio of V_{12}(BmP) over the number of BM is computed, similarly to Clark et al. [11], such ratio roughly results equal to 4.7 cm^3, for HA plans, and to 7.5 cm^3, for

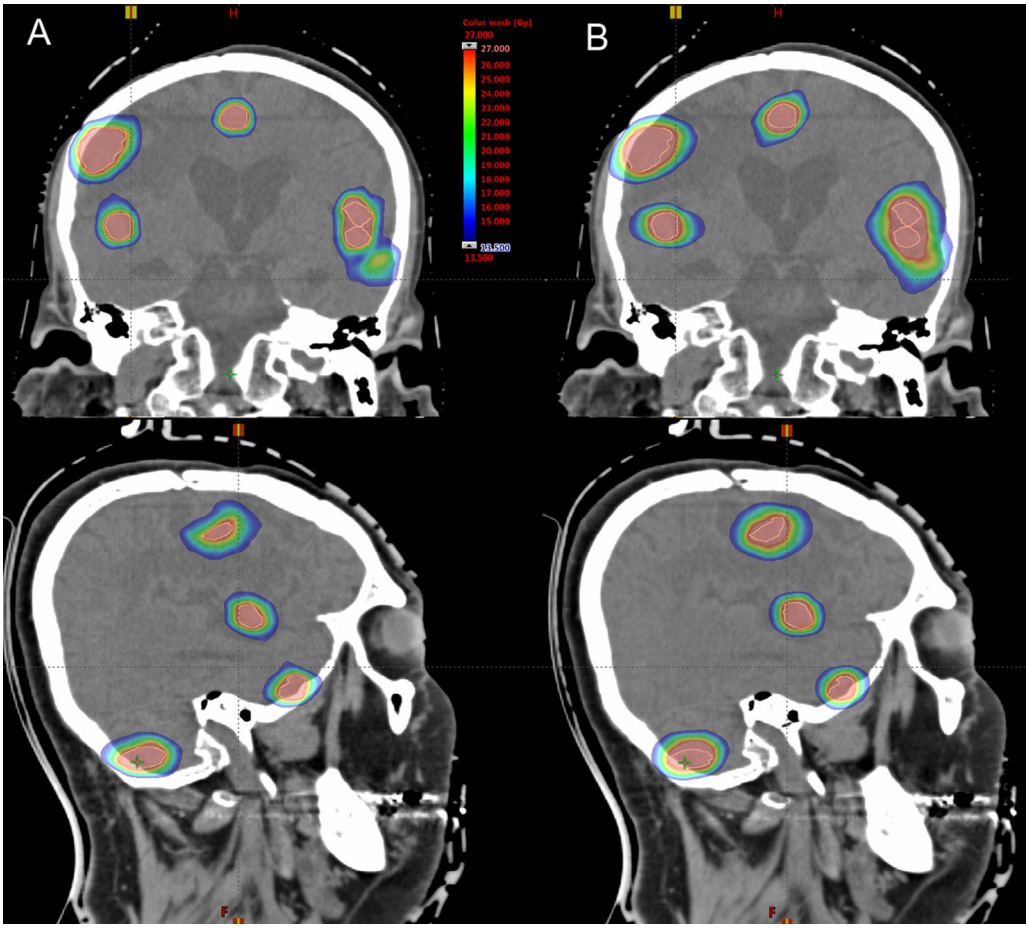

Fig. 6. Coronal (first row) and sagittal (second row) dose distributions for a 10-metastases (outlined in orange) patient (#20), shown in color wash, ranging from 50% to 100% of D_p (D_p = 27 Gy), for the HA (A: first column) and the MBM (B: second column) plans.

MBM plans; thus satisfying the recommended 10 cm^3 threshold. It is noteworthy, although not statistically significant, that HA assured a 37% average reduction in V_{12}(BmP) with respect to MBM. Such difference did not reach statistical significance in our sample, likely because of the huge variability in our PTV_all volumes (0.5–29.0 cm^3) which translated into the wide inter-patient deviation bars in Figs. 3-4A.

As an ancillary comment, at equal angular control point spacing and dose grid step comparable planning times, from 0.5 h until 2–3 h for the most challenging cases (contouring not considered), were needed for both HA and MBM techniques. However, thanks to the included automations, the time actually requiring the planner's attention was rarely greater than 0.5 h.

Dose-delivery accuracy

As secondary aim of the present study, HA and MBM techniques were compared in terms of consistency between computed and measured in-phantom dose distributions. At this purpose, the stringent test criterions of (1 mm, 3%) and (2 mm, 2%) for γ-index computation were adopted, and both local, for (2 mm, 2%), and global, for (1 mm, 3%), normalization of relative DD were performed. Local normalization was used in the commissioning phase of the two TPS. By contrast, global normalization, by mostly weighting the medium-to-high dose range which is of interest for target dose coverage and for the sparing of potentially adjacent critical structures, has become our reference for routine iPDV [29], with a PR^{Max}(1 mm, 3%) $\geq$90% as minimum passing-rate for the clinical usage of the plan.

Although the here reported statistically significant difference in PR^{local}(2 mm, 2%) and PR^{Max}(1 mm, 3%) between the groups of HA and MBM plans, all the plans from both techniques assured PR^{Max}(1 mm, 3%) $\geq$90%. Therefore, we found that both HA and MBM techniques are able to assure an high enough consistency between planned and delivered dose distributions, which is adequate to the SRS/SFRT treatment of multiple BM. About the impact of target geometric complexity, a reduction in passing rates (range: 0.7–1.9%) was associated with an increased number of lesions ($N \geq 4$ vs. $N \leq 3$), for both HA and MBM techniques. Further, by regression analysis, some initial support to the explicative power of Nd_i, as a potential predictor of plan complexity, over PR^{Max}_{HA}(1 mm, 3%) resulted.

In summary, two commercially available mono-isocentric techniques with multiple non-coplanar arcs for linac-based SRS/FSRT of multiple brain lesions were compared both in terms of plan quality and dosimetric accuracy. For plan quality, although HyperArc™ assured a significantly improved target dose conformity (CI), the plans from MultipleBrainMets™ were associated with high enough CI values according to the available literature. For dosimetric accuracy, all plans from both techniques satisfied our test criterion for clinical approval. Hence, both HA and MBM techniques were able to generate high quality plans for SRS/FSRT of multiple BM, which can be performed at the linac within a typical 20 min time slot.

Previous presentation

A previous version of this material was presented as electronic poster at the American Society of Therapeutic Radiation Oncology 60th Annual Meeting in San Antonio, Texas, on October 21–24, 2018.

Authors' contributions

Conception and design: Ruggieri. Anatomical data acquisition: Alongi, Fiorentino, Mazzola, Ricchetti. Dosimetric data acquisition: Naccarato, Ruggieri. Analysis and interpretation of data: Ruggieri. Manuscript preparation: Ruggieri. Manuscript revision: Alongi, Corradini, Fiorentino, Naccarato. All authors read and approved the final manuscript.

Conflict of interest

All authors confirm that the manuscript has not been published elsewhere and is not under consideration by another journal. Further, all authors have approved the manuscript and agree with its submission to *Radiotherapy and Oncology*.

Acknowledgements

Special thanks to Nayef Idrissi and Theresa Hemminger, from Brainlab AG, and to Sylvie Spiessens and Maxime Desplanques, from Varian Medical Systems. Finally, the improvement of the study thanks to the anonymous reviewers is gratefully recognized.

Disclosures

Prof. Alongi, and Dr. Ruggieri served as consultants and received speaker honoraria about the clinical implementation of HyperArc™ from Varian Medical Systems. Prof. Alongi received speaker honoraria from Brainlab AG. The other authors have no personal, financial, or institutional interest in any of the drugs, materials, or devices described in this article.

References

[1] Mehta MP, Tsao MN, Whelan TJ, Morris DE, Hayman JA, Flickinger JC, et al. The American society for therapeutic radiology and oncology (ASTRO) evidence-based review of the role of radiosurgery for brain metastasis. Int J Radiat Oncol Biol Phys 2005;63:37–46.
[2] Nabors LB, Portnow J, Ammirati M, Brem H, Brown P, Butowski N, et al. Central nervous system cancers, version 2.2014. Featured updates to the NCCN Guidelines. J Natl Compr Canc Netw 2014;12:1517–23.
[3] Soffietti R, Kocher M, Abacioglu UM, Villa S, Fauchon F, Baumert BG, et al. A European Organisation for Research and Treatment of Cancer phase III trial of Adjuvant whole-brain radiotherapy versus observation in patients with one to three brain metastases from solid tumors after surgical resection or radiosurgery: quality-of-life result. J Clin Oncol 2013;31:65–72.
[4] Brown PD, Jaeckle K, Ballman KV, Farace E, Cerhan JH, Anderson SK, et al. Effect of radiosurgery alone vs radiosurgery with whole brain radiation therapy on cognitive function in patients with 1 to 3 brain metastases: a randomized clinical trial. JAMA 2016;316:401–9. https://doi.org/10.1001/jama.2016.9839.
[5] Kocher M, Wittig A, Piroth MD, Treuer H, Seegenschmiedt H, Ruge M, et al. Stereotactic radiosurgery for treatment of brain metastases. A report of the DEGRO Working Group on Stereotactic Radiotherapy. Strahlenther Onkol 2014;190:521–32. https://doi.org/10.1007/s00066-014-0648-7.
[6] Nieder C, Grosu AL, Gaspar LE. Stereotactic radiosurgery (SRS) for brain metastases: a systematic review. Radiat Oncol 2014;9:155. https://doi.org/10.1186/1748-717X-9-155.
[7] Lin X, DeAngelis LM. Treatment of brain metastases. J Clin Oncol 2015;33:3475–84. https://doi.org/10.1200/JCO.2015.60.9503.
[8] Yamamoto M, Serizawa T, Shuto T, Akabane A, Higuchi Y, Kawagishi J, et al. Stereotactic radiosurgery for patients with multiple brain metastases (JLGK0901): a multi-institutional prospective observational study. Lancet Oncol 2014;15:387–95.
[9] Alongi F, Fiorentino A, Navarria P, Bello L, Scorsetti M. Stereotactic radiosurgery for patients with brain metastases. Lancet Oncol 2014;15:e246–7.
[10] Clark GM, Popple RA, Young PE, Fiveash JB. Feasibility of single-isocenter volumetric modulated arc radiosurgery for treatment of multiple brain metastases. Int J Radiat Oncol Biol Phys. 2010;76:296–302. https://doi.org/10.1016/j.ijrobp.2009.05.029.
[11] Clark GM, Popple RA, Prendergast BM, Spencer SA, Thomas EM, Stewart JG, et al. Plan quality and treatment planning technique for single isocenter cranial radiosurgery with volumetric modulated arc therapy. Pract Radiat Oncol 2012;2:306–13.
[12] Thomas EM, Popple RA, Wu X, Clark GM, Markert JM, Guthrie BL, et al. Comparison of plan quality and delivery time between volumetric arc therapy (RapidArc) and gamma knife radiosurgery for multiple cranial metastases. Neurosurgery 2014;75:409–17.
[13] Mori Y, Kaneda N, Hagiwara M, Ishiguchi T. Dosimetric study of automatic brain metastases planning in comparison with conventional multi-isocenter

dynamic conformal arc therapy and Gamma knife radiosurgery for multiple brain metastases. Cureus 2016;8:. https://doi.org/10.7759/cureus.882e882.
[14] Ruggieri R, Naccarato S, Mazzola R, Ricchetti F, Corradini S, Fiorentino A, Alongi F. Linac-based VMAT radiosurgery for multiple brain lesions: comparison between a conventional multi-isocenter approach and a new dedicated mono-isocenter technique. Radiat Oncol 2018;13:38. https://doi.org/10.1186/s13014-018-0985-2.
[15] Shaw E, Scott C, Sohuami L, Dinapoli R, Kline R, Loeffler,, et al. Single dose radiosurgical treatment of recurrent previously irradiated primary brain tumors and brain metastases: final report of RTOG protocol 90–05. Int J Radiat Oncol Biol Phys 2000;47:291–8.
[16] Manning MA, Cardinale RM, Benedict SH, Kavanagh BD, Zwicker RD, Amir C, et al. Hypofractionated stereotactic radiotherapy as an alternative to radiosurgery for the treatment of patients with brain metastases. Int J Radiat Oncol Biol Phys 2000;47:603–8.
[17] Sahgal A, Ruschin M, Ma L, Verbakel W, Larson D, Brown PD. Stereotactic radiosurgery alone for multiple brain metastases? A review of clinical and technical issues. Neuro Oncol 2017;19:ii2-ii15. https://doi.org/10.1093/neuonc/nox001.
[18] Fiorentino A, Giaj-Levra N, Tebano U, Mazzola R, Ricchetti F, Fersino S, et al. Stereotactic ablative radiation therapy for brain metastases with volumetric modulated arc therapy and flattening filter free delivery: feasibility and early clinical results. Radiol Med 2017. https://doi.org/10.1007/s11547-017-0768-0.
[19] Roper J, Chanyavanich V, Betzel G, Switchenko J, Dhabaan A. Single isocenter multiple-target stereotactic radiosurgery: risk of compromised coverage. Int J Radiat Oncol Biol Phys 2015;93:540–6. https://doi.org/10.1016/j.ijrobp.2015.07.2262.
[20] Fiorentino A, Tebano U, Sicignano G, Ricchetti F, Di Paola G, Aiello D, et al. Hippocampal dose during linac-based stereotactic radiotherapy for brain metastases: An observational study. Phys Med 2017. https://doi.org/10.1016/j.ejmp.2017.09.129. pii:S1120-1797(17)30452-0.
[21] Morrison J, Hood R, Yin FF, Salama JK, Kirkpatrick J, Adamson J. Is a single isocenter sufficient for volumetric modulated arc therapy radiosurgery when multiple intracranial metastases are spatially dispersed? Med Dosim 2016;41:285–9. https://doi.org/10.1016/j.meddos.2016.06.007.
[22] Ayyangar KM, Jiang SB. Do we need monte carlo treatment planning for linac based radiosurgery? A case study. Med Dosim 1998;23:161–8. https://doi.org/10.1016/s0958-3947(98)00012-0.
[23] Low DA, Harms WB, Mutic S, Purdy JA. A technique for the quantitative evaluation of dose distributions. Med Phys 1998;25:656–61. https://doi.org/10.1118/1.598248.
[24] Clivio A, Vanetti E, Rose S, Nicolini G, Belosi MF, Cozzi L, et al. Evaluation of the machine performance check application for truebeam linac. Radiat Oncol 2015;10:97. https://doi.org/10.1186/s13014-015-0381-0.
[25] Micke A, Lewis DF, Xiang Y. Multichannel film dosimetry with nonuniformity correction. Med Phys 2011;38:2523–34. https://doi.org/10.1118/1.3576105.
[26] Wen N, Lu S, Kim J, Qin Y, Huang Y, Zhao B, et al. Precise film dosimetry for stereotactic radiosurgery and stereotactic body radiotherapy quality assurance using Gafchromic™ EBT3 films. Radiat Oncol 2016;11:132. https://doi.org/10.1186/s13014-016-0709-4.
[27] Hilman Y, Kim J, Chetty I, Wen N. Refinement of MLC modeling improves commercial QA dosimetry system for SRS and SBRT patient-specific QA. Med Phys 2018;45:1351–9. https://doi.org/10.1002/mp.12808.
[28] Lilliefors HW. On the Kolmogorov-Smirnov test for normality with mean and variance unknown. J Amer Stat Assoc 1967;62:399–402.
[29] Miften M, Olch A, Mihailidis D, Moran J, Pawlicki T, Molineu A, et al. Tolerance limits and methodologies for IMRT measurement-based verification QA: Recommendations of AAPM Task Group No. 218. Med Phys 2018;45:e53–83. https://doi.org/10.1002/mp.12810.
[30] Flickinger JC, Lundsford LD, Kondziolka D, Maitz AH, Epstein AH, Simons SR, et al. Radiosurgery and brain tolerance: An analysis of neurodiagnostic imaging changes after gamma knife radiosurgery for arteriovenous malformations. Int J Radiat Oncol Biol Phys 1992;23:19–26.
[31] Korytko T, Radivoyevitch T, Colussi V, Wessels BW, Pillai K, Maciunas RJ, et al. 12 Gy gamma knife radiosurgical volume is a predictor for radiation necrosis in non-AVM intracranial tumors. Int J Radiat Oncol Biol Phys 2006;64:419–24.
[32] Blonigen BJ, Steinmetz RD, Levin L, Lamba MA, Warnick RE, Breneman JC. Irradiated volume as a predictor of brain radionecrosis after linear accelerator stereotactic radiosurgery. Int J Radiat Oncol Biol Phys 2010;77:996–1001.
[33] Paddick I, Lippitz B. A simple dose gradient measurement tool to complement the conformity index. J Neurosurg 2006;105:194–201.
[34] Jang SY, Lalonde R, Ozhasoglu C, Burton S, Heron D, Huq MS. Dosimetric comparison between cone/Iris-based and InCise MLC-based CyberKnife plans for single and multiple brain metastases. J Appl Clin Med Phys 2016;17:184–99.
[35] Molinier J, Kerr C, Simeon S, Ailleres N, Charissoux M, Azria D, et al. Comparison of volumetric-modulated arc therapy and dynamic conformal arc treatment planning for cranial stereotactic radiosurgery. J Appl Clin Med Phys 2016;17:92–101. https://doi.org/10.1120/jacmp.v17i1.5677.
[36] Liu H, Andrews DW, Evans JJ, Werner-Wasik M, Dicker AP, Shi W, et al. Plan quality and treatment efficiency for radiosurgery to multiple brain metastases: non-coplanar Rapidarc vs Gamma Knife. Front Oncol 2016;6:26. https://doi.org/10.3389/fonc.2016.00026.
[37] Ballangrud Å, Kuo LC, Happersett L, Lim SB, Beal K, Yamada Y, et al. Institutional experience with SRS VMAT planning for multiple cranial metastases. J Appl Clin Med Phys 2018;19:176–83. https://doi.org/10.1002/acm2.12284.